Thermal and Structural Considerations in the Design of a Rankine Vapor Microturbine

Mokhtar Liamini[1], Hassan Shahriar[2], Srikar Vengallatore[2], Luc G. Fréchette[1]
[1]Department of Mechanical Engineering, University of Sherbrooke, Sherbrooke, Canada
[2]Department of Mechanical Engineering, McGill University, Montreal, Canada

Abstract: This paper reports a global modeling and design approach to design a Rankine Microturbine for micro power generation from waste heat. The primary performance metrics and design challenges were identified, and models were developed for conjugate thermal and structural analyses. The results of these models, and their implications for size, shape, and materials selection, are presented. The need for low conductivity materials for the rotor and static structure of the microturbine is highlighted and a viable device configuration is proposed for elevated temperature operation.

Key words: Microturbine; Micro heat engine; Design; Heat transfer; Thermomechanical stresses.

1. INTRODUCTION

Among the many devices currently under development for portable power generation is the Rankine Vapor Microturbine. The first demonstration of the core microturbopump for such an engine was reported in 2006, and consisted of a five layer stack (with four silicon wafers and one glass wafer) [1]. This device was operated with air at ambient temperature to assess the performance of the turbine, pump, seals and bearings. The goal for the next generation of devices is to use water and steam as the working fluids, which implies operation at higher temperatures of a few hundred degrees centigrade. Figure 1 shows a schematic cross-section of this device. The rotor (1) is held in place using thrust bearings (2) and a journal bearing (3). The evaporator (4) is separated from the condenser (5) by a static structure (6). The pump (7) is located underneath the rotor, and generators (8) are integrated into the stationary and rotating structures to generate electricity.

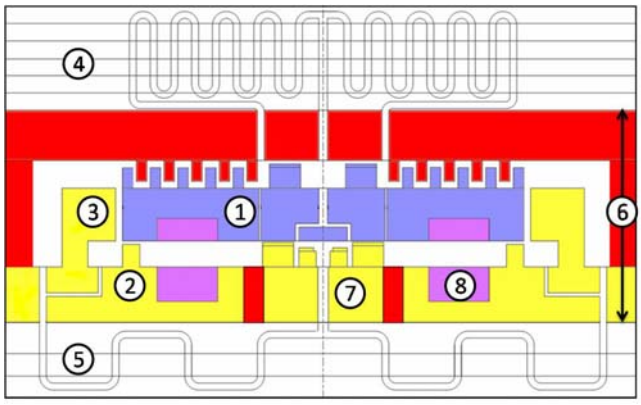

Fig. 1: Schematic cross-section of a Rankine microturbine: (1) rotor, (2) thrust bearing, (3) journal bearing, (4) evaporator, (5) condenser, (6) static structure, (7) pump, and (8) generator. The structure is ~1 mm in thickness and ~10 mm in diameter.

2. GOALS AND DESIGN CHALLENGES

The Rankine Microturbine utilizes the Rankine vapor power thermodynamic cycle to convert heat to mechanical power. To maximize power generation, the performance goals are: (i) increase the power output by increasing the temperature difference between the inlet and outlet of the turbine; (ii) increase the power output by increasing the pressure ratio of the pump; and (iii) maximize the power output per unit surface area for efficient miniaturization.

The performance goals are limited by operating conditions (evaporator and condenser temperatures, and internal pressure), available fabrication techniques, and reliability issues. For given operating conditions, the device can experience unwanted heat leakage (due to temperature gradients in excess of 100^{o}C/mm), thermomechanical stresses (due to differential expansion), and unwanted boiling or condensation of the working fluid. The parameters that allow us to address these challenges are component geometry, layout, and choice of materials used for the device.

We present here an integrated approach for thermal and structural analyses, following which we propose a device configuration in order to achieve our performance goals.

3. THERMAL ANALYSIS

The primary goal of the thermal analysis is to evaluate the impact of undesirable heat leakage on the performance of the engine. To this end, we use a hierarchy of models of different levels of complexity for heat transfer. This approach can be readily extended to other microdevices that operate under large temperature gradients.

As a first step, the various paths through which heat

leakage can occur are identified. For the Rankine Microturbine, this includes the static structure surrounding the rotor, the rotor itself, and laterally between the bearings, seals, and pump (Fig 1). The thermal behaviour of each component is analyzed below.

3.1 Modeling of the Static Insulator

Heat leakage through the static structure will be dominated by the thermal resistance of the walls surrounding the rotor. Heat that directly conducts through the structures, without doing work in the turbine, leads to a direct reduction of the overall thermal efficiency of the device. Figure 2 illustrates this impact as a function of the wall thermal resistance. Design spaces are shown for single-crystal silicon and amorphous silicon dioxide (fused silica) by estimating the thermal resistance of the walls using a one-dimensional (1D) model, $R_{th} = L/kA$, where L is the thickness of the rotor, k is the thermal conductivity of the wall material, and A is the effective cross-sectional area of the walls. This simple model leads to the profound design implications that silicon is not a viable material. Instead, structural materials with low thermal conductivity are required.

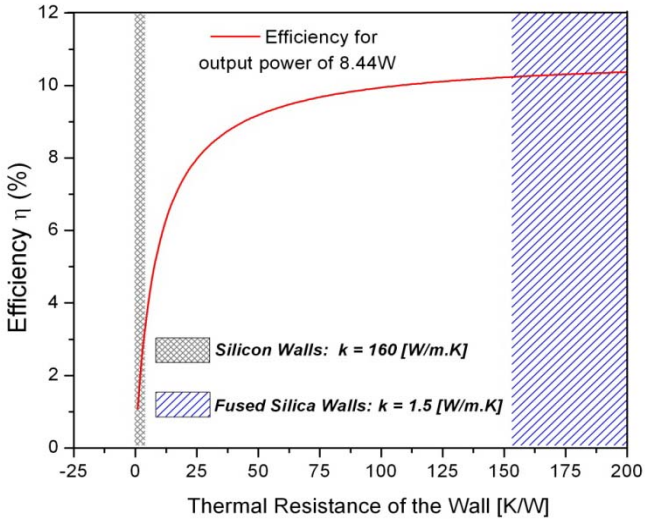

Fig. 2: Effect of the thermal resistance of the static walls on the thermal efficiency of a Rankine microturbine, showing that low conductivity materials (such as fused silica) are required for acceptable device efficiency.

3.2 Modeling of the Rotor

To predict the heat transfer in the turbine, we coupled a finite element model for the meshed rotor with lumped models for the various components surrounding the rotor, as shown in Fig. 3. The FEM calculations were implemented with COMSOL, which was then linked with MATLAB functions that represent the surrounding components.

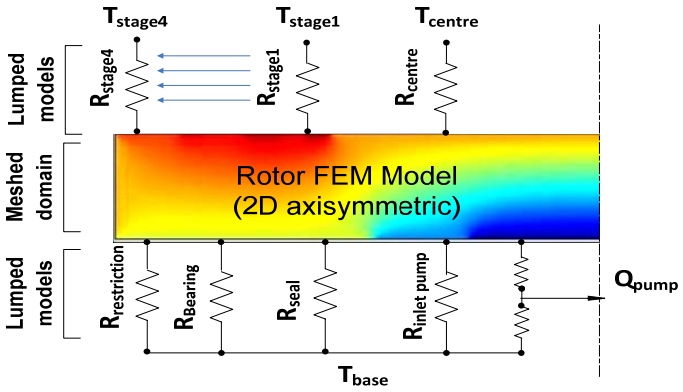

Fig. 3: Scheme of coupled heat transfer model approach consisting of discretized FEM for the rotor surrounded by lumped models for the components.

A description of the various components and the type of models used for heat transfer are tabulated in Table 1 and briefly summarized below. The analysis is iterative and convergence was achieved once the temperatures and heat fluxes stabilized. This approach enabled quick calculations to be carried out to define the guidelines for the device layout and for materials selection.

Table 1: Description of models used for the various components

	Ext. Flow	Int. Flow	Numerical	Analytical	Heat Conduction
Centre of Pump & Turbine [3]	■		■		
Flat Surface of Rotor [4]	■		■		
Rotor Blades [5]	■		■		
Pump		■	■		
Seal, Generator, Restrictor		■		■	
Journal Bearing				■	■
Rotor			■		■

The model for the centre of the turbine and pump was adopted from the literature on flows over rotating disks. This model was used after validating it for several fluids and different Prandtl numbers. The turbine itself was divided into bladed zones and flat zones. The former was modeled using boundary layer theory assuming steady, incompressible, laminar flow uniform surface temperature; and no pressure gradient. Comparison between conduction in the blades and convection at the blade surface shows the former to be dominant. Hence, the blades were assumed to be isothermal, and were taken into account mainly as an increase of surface area. For the pump, generator, seals, journal bearings, and restrictor, the governing equations are based on momentum and energy conservation, with the assumption of stable, incompressible, laminar and developed flows.

3.3 Results and Discussion

The models described above represent a trade-off between accuracy and convenience for this specific stage of design. Parametric studies were performed to

examine the effects of different variables on efficiency and maximum pump temperature. Fig. 4 shows representative results for the efficiency and maximum pump temperature as functions of the thermal resistance of the rotor.

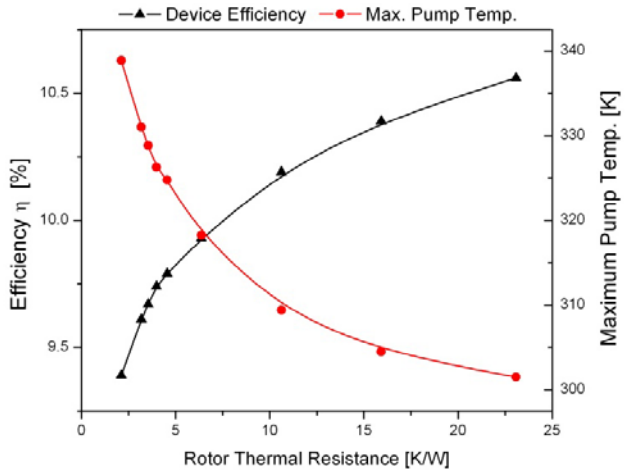

Fig. 4: Effect of the rotor thermal resistance on the thermal efficiency and the maximum pump temperature.

The thermal resistance of the rotor was varied between 2 and 25 K/W that, for a rotor of typical dimensions, represents a thermal conductivity ranging from 1 to 12 W/m.K. Fig. 4 shows that the impact on efficiency is not significant, but the pump temperature rapidly increases towards the boiling temperature. These results suggest that insulating materials, rather than single crystal silicon, should be used for the rotor.

4. STRESS ANALYSIS

4.1 Modeling of the Static Insulator

The static insulator of the Rankine microengine is modeled as a cylindrical pressurized chamber with flat ends. This structure is crucial to both the thermal management and the mechanical integrity of the device. The mechanical stresses generated in the static insulator are functions of geometry, material properties, and steady state operating conditions. These stresses were analyzed using a 2D plane-stress thermoelasticity model and an axisymmetric finite element analysis.

Based on plane strain elasticity equations [6], the mechanical stress component has its maxima at the internal radius. For an internal pressure, P, we can express the dimensionless Von Mises elastic stress as:

$$\frac{\sigma}{P}=\left[\frac{1-4\nu+4\nu^2+3\xi^4}{\left(\xi^2-1\right)^2}\right]^{\frac{1}{2}} \qquad (1)$$

Here, ν is Poisson's ratio and ξ is the ratio of outer radius to inner radius ($\xi = r_o/r_i$). Similarly the dimensionless Von Mises thermal stress due to a temperature gradient ΔT between the inner and outer radii is given by:

$$\frac{\sigma}{\left(\frac{E\alpha\Delta T}{1-\nu}\right)}=\left[\frac{1}{4\left[\ln(\xi)\right]^2}-\frac{1}{\ln(\xi)}\left(\frac{\xi^2}{\xi^2-1}\right)+\frac{\xi^4}{\left(\xi^2-1\right)^2}\right]^{\frac{1}{2}} \qquad (2)$$

During steady state operation, ΔT is on the order of a few Kelvin. Fig. 5 shows the dimensionless stresses as a function of ξ. The thermal stresses are considerably smaller than the mechanical stresses, and a ratio of radii exceeding 1.1 ensures a sufficient decrease in the mechanical stress.

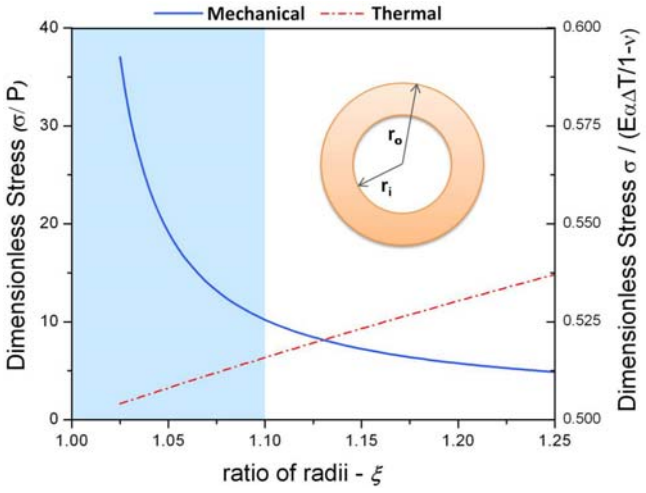

Fig. 5: Variation of thermal and mechanical stress as a function of the ratio of radii.

While the 2D plain-strain analysis provides us with a design range for insulator thickness, it fails to capture the edge stresses for this *short* cylinder. The edge stresses were evaluated using a coupled thermomechanical finite-element model in COMSOL. The model reveals that edge stresses are the dominant stresses in the entire structure. In Fig. 6 we see a schematic of the model (left) and the finite element results (right). A fillet was introduced at the edge to reduce the stress concentration. A fillet radius of 5 µm produces a maximum stress of 156 MPa while a 20 µm radius reduces that stress to 74 MPa. We also see that the maximum deflection in the static structure for the given conditions is 1.7µm which would incur a significant change in the thrust bearing, pump, and seal gaps. The finite element results require the structural materials to withstand the above sustained stress and have very low thermal expansion coefficients. The materials must also be amenable to microfabrication, and preferably allow the formation of fillets.

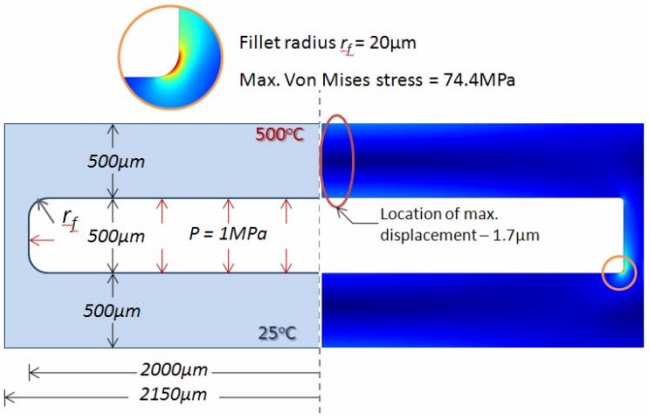

Fig. 6: Schematic and results of a coupled thermal & mechanical finite element model of a fused silica static structure.

5. SELECTION OF STRUCTURAL MATERIALS

The models for thermal and mechanical behavior of the different components can be used to identify material indices by following the approach of Ashby [7]. The four material indices that should be maximized for this system are:

$$M_1 = \frac{\sigma_y}{k};\ M_2 = \frac{\sigma_f}{k};\ M_3 = \frac{\sigma_y}{E\alpha};\ M_4 = \frac{\sigma_f}{E\alpha}$$

Here, σ_y is the yield strength, σ_f is the fracture strength, E is the Young's modulus, and α is the coefficient of thermal expansion. Using material selection charts and high-temperature thermal conductivity values [8], three optimal candidates were identified: yttria-stabilized zirconia (YSZ), fused silica, and quartz. Table 2 highlights the properties of these materials at ambient conditions.

Table 2: Properties of candidate materials (Source: Cambridge Engineering Selector)

Properties		YSZ	Silica	Quartz
Fracture Strength	**[MPa]**	771	198	144
Young's Modulus	**[GPa]**	199	74	76
Thermal Conductivity	**[W/mK]**	2	1.5	8

Among these candidates, fused silica is the most promising in terms of fabrication. Advanced Oxide Etch tools, laser micromachining, and wet etching of fused silica have been demonstrated, although with various degrees of success for the required high aspect ratio geometries.

6. RECOMMENDATIONS AND CONCLUSIONS

The next generation Rankine Microturbine will need to reduce the thermo mechanical challenges by integrating low conductivity materials and choosing a layout that minimizes the thermal gradients. It will consist of a multi-spooled configuration with four

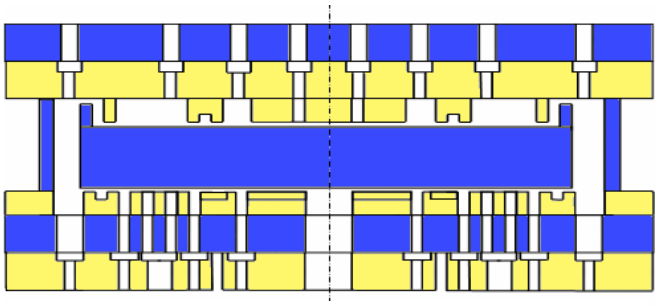

Fig. 7: Schematic representation of the turbine holding the pump, fused silica is in blue, silicon is in yellow

microturbine rotors arranged in series. The last of these turbines, exposed to lower temperature steam, drives the pump while the others generate power. This configuration can achieve high pressure expansions for greater efficiency while maintaining the power to surface area ratio. The turbopump configuration shown in Fig. 7 is a six wafer stack that combines the required insulation (fused silica) and ease of fabrication (silicon) for these complex structures. Thermo-mechanical stress must be considered, both to prevent mechanical failure and maintain the small tolerances. Specifically, edge fillets are desirable to address the high stresses in the corners of the pressurized static structure. This work paves the way for the detailed design and the fabrication of a demo microturbopump to be operated at high temperatures and pressures.

ACKNOWLEDGMENTS

This work was supported by the National Sciences and Engineering Research Council (NSERC) of Canada and General Motors of Canada. Technical discussions with Dr. Carlton Fuerst and Dr. Jihui Wang are gratefully acknowledged.

REFERENCES

[1] Lee C, Liamini M, Fréchette L G, *Design, Fabrication, and Characterization of a Microturbopump for a Rankine Cycle Micro Power Generator,* **Proc. 2006** Solid State Sensor, Actuator, and Microsystem Workshop, Hilton Head Island, SC, June 4-8 2006.

[2] Epstein, et al. 1997 *Micro-Heat Engines, Gas Turbines, and Rocket Engines*, **AIAA 97-1773**.

[3] Dorfman L A 1963, *Hydrodynamic Resistance and Heat Loss from Rotating Solids,* Oliver and Boyd, Edinburgh and London.

[4] Kays W M, Crawford M E 2005, *Convective heat and Mass Transfer* McGraw-Hill.

[5] Incropera F P, DeWitt D P 2002, *Introduction to Heat Transfer*, Fourth Edition, Wiley.

[6] Sadd, Martin H. 2005, *Elasticity, Theory, Applications and Numerics.* ELSEVIER Butterworth-Heinemann

[7] Ashby, Michael, 2005, *Material Selection in Mechanical Design.* Butterworth-Heinemann

[8] W.D. Kingery, J. Francl, R. L. Colbe, and T. Vasilos, "*Thermal Conductivity: X, Data for Several Pure Oxide Materials Corrected to Zero Porosity*," J. Am. Ceram. *Soc.,* 37 [2,Part II] 107-110 (1954)